SLUJST
Sule Lamido University Journal of Science & Technology Vol. 9 No. 1&2 [May, 2024], pp. 149-158
https://doi.org/10.56471/
Online ISSN: 2736-0903
Print ISSN: 2736-089X
www.slujst.edu.ng

Experimental and Theoretical Investigation on Physio-Mechanical Features of Calcium Sulfo-Phospho-Borate Glasses Containing Dy^{3+} Ions

Ibrahim Mohammed Danmallam[1], Suleiman Bashir Adamu[2] and Ibrahim Bulus[3]

[1]Sokoto Energy Research Centre, Usmanu Danfodiyo University, Sokoto, Nigeria
[2]Department of Physics, Faculty of Natural and Applied Sciences, Sule Lamido University, 048 Kafin Hausa. Jigawa State, Nigeria.
[3]Department of Physics, School of Sciences, Kaduna State College of Education Gidan waya, Kafanchan, Nigeria.

*Corresponding author email: ibrahimdanmallam@gmail.com

Abstract

This study investigates the incorporation of varying amounts of Dy^{3+} into calcium sulfo-phospho-borate glass using the melt-quenching method. The resulting glasses were analyzed to explore how Dy^{3+} affects their physical and mechanical properties. Furthermore, the correlation between experimentally measured and theoretical mechanical features was examined. As the concentration of Dy^{3+} increased, the density of the glass rose from 3.387 to 3.646 g/cm^3, indicating network shrinkage and enhanced compactness. Ultrasonic velocities (both longitudinal and shear) were found to improve, ranging from 4565 to 4700 m/s and 2294 to 2359 m/s, respectively. Additionally, the elastic moduli (including Young's modulus, longitudinal modulus, shear modulus, and bulk modulus) increased with higher Dy^{3+} ion content. Experimental measurements of the elastic moduli aligned well with predictions from the Makishima-Mackenzie and Rocherulle models. Moreover, Poisson's ratio decreased from 0.331 to 0.270, while Vickers hardness values increased from 2.009 to 4.517 GPa. These results underscore the necessity of calculating the ultrasonic and mechanical properties of the glasses. This investigation suggests that the studied glass holds potential for use in hard surface engineering applications.

Keywords: *Dysprosium ions, Elastic moduli, Ultrasonic pulse-echo technique; Makishima Mackenzie, Rocherulle model.*

1. Introduction

Recent studies have extensively explored the incorporation of rare earth (RE) ions into glass matrices due to their wide-ranging applications in fiber optics, fiber lasers, solid-state lasers, and communications (Bengisu et al., 2016; Razak et al., 2016; Karthikeyan et al., 2018; Adamu et al., 2022a). Oxide glasses, in particular, have garnered significant attention due to their superior mechanical properties, including higher elastic strain limits, hardness, resistance to abrasion, and overall strength (Halimah et al., 2018; Cheong et al., 2022). The chemical composition of the glass matrix profoundly influences the physical and mechanical characteristics of both the modifiers and rare earth ions, as evidenced in the literature (Abdullahi et al., 2020; Danmallam et al., 2021; Adamu et al., 2022a).

Phosphate-based glasses, known for their exceptional ultraviolet (UV) transmittance, mechanical properties, low viscosity, high transparency, isotropic refractive index, thermal stability, and ease of fabrication, hold promise for diverse applications (Danmallam & Bulus, 2020; Alqarni et al., 2020 Alharshan et al., 2022). However, despite their numerous advantages, they suffer from certain limitations such as poor chemical resistance, which can be addressed by introducing metallic oxides like ZnO and MgO (Danmallam et al., 2021). Rare earth ions, such as Dysprosium, exhibit consistent oxidation states and possess high luminescent properties depending on the

Online ISSN: 2736-0903
Print ISSN: 2736-089X
www.slujst.edu.ng

surrounding structural geometry. Dysprosium-doped glasses offer remarkable features such as high resistance, hardness, and low fracture toughness (Halimah et al., 2018). Several authors advocate for the use of Vickers indentation hardness as the preferred technique for assessing the mechanical parameters of bulk materials, wherein a fixed load is applied to a diamond indenter and evaluated under a microscope (Bengisu et al., 2016; Danmallam et al., 2021; Yaacob et al., 2023).

Considering these advantages, the main objectives of this study are (i) to synthesize calcium sulfo-phospho-borate glasses doped with Dy3+ ions, (ii) to assess the influence of Dysprosium oxide concentration on the physical properties of the glasses, (iii) to determine the experimental mechanical properties of the glasses, and investigate theoretical predictions using the Makishima-Mackenzie and Rocherulle models, and (iv) to establish correlations between the experimental and theoretical mechanical attributes of the glasses.

2. Materials and Methods

2.1 Sample Preparation

A series of dysprosium ion-doped calcium sulfo-phospho-borate glasses, denoted as CSPBDy with mol% x = 0.2, 0.4, 0.6, 0.8, and 1.0, were synthesized using the melt-quenching technique. The starting chemical constituents, including calcium oxide (CaO), dysprosium oxide (Dy_2O_3), boric acid (H_3BO_3), sulfuric acid (H_2SO_4), and phosphoric acid (H_3PO_4), obtained from Sigma Aldrich with a purity of 99.99%, were used. The glass samples' codes and compositions are detailed in Table 1. Approximately 15g batches of the compositional mixtures were thoroughly mixed in a porcelain crucible and weighed accordingly. The resulting mixture was gradually heated to 300°C, over 45 minutes in an electric furnace to facilitate the dehydration of water (H_2O) and carbon dioxide (CO_2). Subsequently, the furnace temperature was incrementally raised at a rate of 25°C/min to 950°C and maintained for 1 hour. To alleviate any strain, the resulting bubble-free molten glass was promptly transferred to a secondary furnace and annealed at 350°C for 3 hours.

Table 1. Sample nomination and composition (mol%) of CSPBDy glass system.

S/N	Glass sample code	Glass composition (mol %)				
		B_2O_3	SO_3	P_2O_5	CaO	Dy_2O_3
1	CSPBDy0.2	39.8	20	30	10	0.2
2	CSPBDy0.4	39.6	20	30	10	0.4
3	CSPBDy0.6	39.4	20	30	10	0.6
4	CSPBDy0.8	39.2	20	30	10	0.8
5	CSPBDy1.0	39.0	20	30	10	1.0

2.2 Sample Characterization

2.2.1 X-Ray Diffraction Measurement

To affirm the non-crystalline structure of the synthesized CSPBDy glasses, we employed a Siemens X-Ray Diffractometer (model, D5000) outfitted with Cu-Kα radiation (wavelength, λ≈1.54 Å) and powered by a 40 kV, 30 mA source. Powder X-ray diffraction analyses were carried out across a 2θ range of 10° to 80° at a scanning rate of 2° per minute, following the methodology outlined in our previous study (Danmallam et al., 2021).

2.2.2 Physical Properties

The density of the samples was determined using an electronic densimeter (MD-300S) following the Archimedes principle, with distilled water serving as the submerging liquid at room temperature, as described in detail by Tafida et al. (2024). The densities (ρ) of the CSPBDy glasses and their molar volumes were estimated using the provided Equations (1) and (2), as governed by:

Sule Lamido University Journal of Science & Technology Vol. 9 No. 1&2 [May, 2024], pp. 149-158
https://doi.org/10.56471/
Online ISSN: 2736-0903
Print ISSN: 2736-089X
www.slujst.edu.ng

$$\rho = \frac{M_a}{V} \quad (1)$$

$$V_m = \frac{M_w}{\rho} \quad (2)$$

where V denotes the volume of the glass sample, while M_a stands for the mass of the glass sample in the air, M_w with represents the molecular weight of the host glass. Additionally, various physical parameters are assessed, including ion concentration, inter-ionic distance, field strength, and Polaron radius.

2.2.3 Mechanical Properties

The ultrasonic pulse-echo method is frequently employed as a non-destructive testing technique to investigate the acoustic properties of glass materials (Danmallam et al., 2021; Cheong et al., 2022). Utilizing this method, the propagation time of acoustic waves was measured at 5 MHz using the Ritec Ram-5000 Snap. Subsequently, the ultrasonic velocity was determined based on the established relationships (Adamu et al., 2022a):

$$v = {}^{2x}\!/_{\Delta t} \quad (3)$$

where v represents the ultrasonic velocity, including both longitudinal (v_L) and shear (v_S) velocities, x denotes the thickness of the glass, and Δt signifies the difference in time of flight. Subsequently, the ultrasonic velocity and density of the glass were utilized to estimate the experimental elastic moduli (including longitudinal modulus, L_{exp}; shear modulus, G_{exp}; Young's modulus, E_{exp}; and bulk modulus, K_{exp}) as well as Poisson's ratio (σ_{exp}) of the glasses. The elastic moduli and microhardness ($H_{\exp}$) of CSPBDy glasses are computed using Equations (4) to (9) (Adamu et al., 2022a):

$$L_{\exp} = \rho v_L^2 \quad (4)$$

$$G_{\exp} = \rho v_S^2 \quad (5)$$

$$K_{\exp} = L_{\exp} - \left({}^{4}\!/_{3}\right) G_{\exp} \quad (6)$$

$$E_{\exp} = 2(1+\sigma_{\exp}) G_{\exp} \quad (7)$$

$$\sigma_{\exp} = \frac{\left(L_{\exp} - 2G_{\exp}\right)}{2\left(L_{\exp} - G_{\exp}\right)} \quad (8)$$

$$H_{\exp} = \frac{\left(1-2\sigma_{\exp}\right) E_{\exp}}{6\left(1+\sigma_{\exp}\right)} \quad (9)$$

where the elastic moduli measurements are in (GPa) units.

2.3 Theoretical Models

2.3.1 Makishima and Mackenzie and Rocherulle Models

Makishima and Mackenzie (MM) introduced a theoretical calculation model in 1975 for determining the chemical composition of oxide glasses. This model relies exclusively on the dissociation energy of the oxide constituents per unit volume and packing density of these constituents (Adamu et al., 2022a; Tafida et al., 2024). For multicomponent glasses, the MM model provides equations for the bulk (K_{MM}), Young's

SLU JST
Sule Lamido University Journal of Science & Technology Vol. 9 No. 1&2 [May, 2024], pp. 149-158
https://doi.org/10.56471/
Online ISSN: 2736-0903
Print ISSN: 2736-089X
www.slujst.edu.ng

modulus (E_{MM}), shear modulus (G_{MM}), and Poisson's ratio the (σ_{MM}) as outlined below (Tafida et al., 2024):":

$$K_{MM} = 1.2 V_t E_{MM} \tag{10}$$

$$E_{MM} = 2 V_t G_t \tag{11}$$

$$G_{MM} = \frac{3 K_{MM} E_{MM}}{\left(9 K_{MM} - E_{MM}\right)} \tag{12}$$

$$\sigma_{MM} = \left(\frac{E_{MM}}{2 G_{MM}} - 1\right) \tag{13}$$

where x_i signifies the mole fraction of the component, ρ represents the density of the glass, M_w stands for the effective molecular weight of the chemical composition, G_t denotes the dissociation energy, and V_t represents the packing density. These variables are defined by the following relationships:

$$V_t = \left(\frac{\rho}{M_w}\right) \sum_i V_i x_i \tag{14}$$

$$G_t = \sum_i G_i x_i \tag{15}$$

The Rocherulle model presents an alternative approach to elastic properties in glasses. It proposes that the elastic moduli are independent of the material's density (Rocherulle et al., 1989;Tafida et al., 2024). According to the same reference, theoretical elastic moduli (bulk modulus, shear modulus, Young's modulus) can be determined using Equations (16) to (19) as follows:

$$K_{thR} = 1.2 C_t E_{thR} \tag{16}$$

$$E_{thR} = 2 C_t \sum_i G_t x_i \tag{17}$$

$$G_{thR} = \frac{3 K_{thR} E_{thR}}{\left(9 K_{thR} - E_{thR}\right)} \tag{18}$$

$$\sigma_{thR} = \left(\frac{E_{thR}}{2 G_{thR}} - 1\right) \tag{19}$$

where C_i denotes the packing factor for each oxide and C_t denotes the total packing density given by the relations:

$$C_i = \frac{4\pi}{3} \frac{\rho N_A}{M_w} \left(m R_A^3 + n R_O^3\right) \tag{20}$$

$$C_t = \sum_i C_i x_i \tag{21}$$

3. Results and Discussion

3.1 XRD Analysis

The X-Ray Diffraction spectra of the examined glasses are depicted in Figure 1. Evidently, the spectra exhibit characteristic diffuse bands typical of XRD patterns observed in amorphous materials. The absence of any crystal

Sule Lamido University Journal of Science & Technology Vol. 9 No. 1&2 [May, 2024], pp. 149-158
https://doi.org/10.56471/
Online ISSN: 2736-0903
Print ISSN: 2736-089X
www.slujst.edu.ng

peaks, but rather broad humps occurring at 2θ ≈ 5°–10° and 15°–25°, confirms the amorphous nature of the CSPBDy glass samples produced.

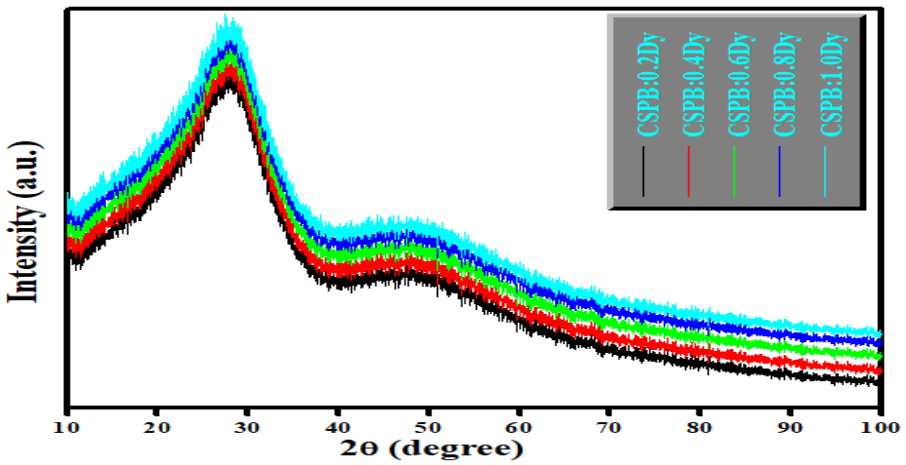

Figure 1: XRD pattern of CSPBDy glasses.

3.2 Physical Properties

The physical characteristics of CSPBDy glasses are assessed using established physical relationships. Parameters such as density serve as a basis for deriving additional physical properties, including molar volume, ion concentration, inter-ionic distance, field strength, and Polaron radius. Density provides essential information regarding the compactness of the network and the coordination number of atoms within the rigid amorphous matrix (Halimah et al., 2018). The densities ranged from 3.387 to 3.774 g/cm³, while the molar volume decreased from 40.180 to 30.281 cm³ with an increase in Dy^{3+} ion content. This variation affects the polarization factor and consequently the field strengths (Danmallam & Bulus, 2020).

Table 2. The physical parameters of CSPBDy glasses

Physical Properties	CSPBDy0.2	CSPBDy0.4	CSPBDy0.6	CSPBDy0.8	CSPBDy1.0
Density (g.cm^{-3}) (±0.003)	3.387	3.460	3.536	3.646	3.774
Molar volume (cm^3) (±0.03)	40.180	39.584	38.980	37.963	30.281
Dy^{3+} ions concentration (×10^{22} ion.cm^{-3}) (±0.003)	1.049	1.521	2.008	2.379	1.591
Polaron radius (Å (±0.008)	1.873	1.655	1.509	1.426	1.602
Inter ionic Distance (Å) (±0.067)	4.646	4.105	3.743	3.537	3.976
Field strength (×10^{17} cm^{-2}) (±0.005)	1.796	2.300	2.767	3.098	2.337

3.3 Mechanical Properties

3.3.1 Ultrasonic Velocities and Elastic Properties

In a broader context, understanding the elastic parameters of RE^{3+} doped glass systems hold significant importance for deciphering their structural arrangements and for applications such as glass fiber fabrication (Bengisu, 2016). The dependency of ultrasonic velocities (longitudinal (v_L) and shear (v_S)) and the computed elastic moduli, along with their derivatives, is summarized in Table 3. As evident from the density results, the introduction of Dy^{3+} dopant into the CSPBDy network results in a denser and more rigid structure. In this investigation, both velocities v_L and

SLUJST
Sule Lamido University Journal of Science & Technology Vol. 9 No. 1&2 [May, 2024], pp. 149-158
https://doi.org/10.56471/
Online ISSN: 2736-0903
Print ISSN: 2736-089X
www.slujst.edu.ng

v_S exhibited an increase from 4565 to 4700 m/s and 2294 to 2359 m/s, respectively. Particularly, the rise in ultrasonic velocity values, depicted in Figure 3(a), is attributed to the increased number of bridging oxygen (BO) and consequently improved connectivity within the glass network (Bulus et al., 2017; Danmallam et al., 2021). This finding further confirms that the addition of Dy_2O_3 to CSPBDy glass facilitates the rapid propagation of ultrasonic waves within the glass structure.

On the contrary, elastic moduli, which represent the stiffness of a material, are determined by the bonding strength between its atoms. Consequently, a higher value of elastic moduli indicates greater material stiffness (Alharshan et al., 2022; Tafida et al., 2024). As evident from Table 3 and Figure 3(b), it is apparent that the elastic moduli of our fabricated CSPBDy glasses increase with Dy2O3 content. Additionally, the observation of a relatively higher value of E_{exp} compared to K_{exp} suggests that these glasses can endure higher longitudinal stress than transverse stress. Notably, the density, ultrasonic velocities, and elastic moduli all uniformly increase with higher Dy_2O_3 content, indicating the significant role of fused Dy_2O_3 in strengthening the glass network. On the other hand, Poisson's ratio (σ) for any structure is the ratio of lateral to longitudinal strain under applied tensile forces, revealing variations in the dimension of the network structure (Adamu et al., 2022a; Alharshan et al., 2022). The obtained values of σ_{exp} for the corresponding CSPBDy glass samples are 0.331, 0.331, 0.329, and 0.332. These values closely match those of pure B_2O_3 glass, which has a Poisson's ratio of 0.3 and is characterized by a 2D layer structure (Adamu et al., 2022a). Additionally, microhardness is another notable mechanical property of solids, defined as the resistance to permanent indentation (Danmallam et al., 2021). The evaluated microhardness (H_{exp}) values follow a similar trend as the elastic moduli, ranging between 2.009 and 4.517 GPa, indicating an overall increase in the stiffness (rigidity) of the glass network. Furthermore, a comparison between the elastic data from this study and those reported for other glasses is summarized in Table 3.

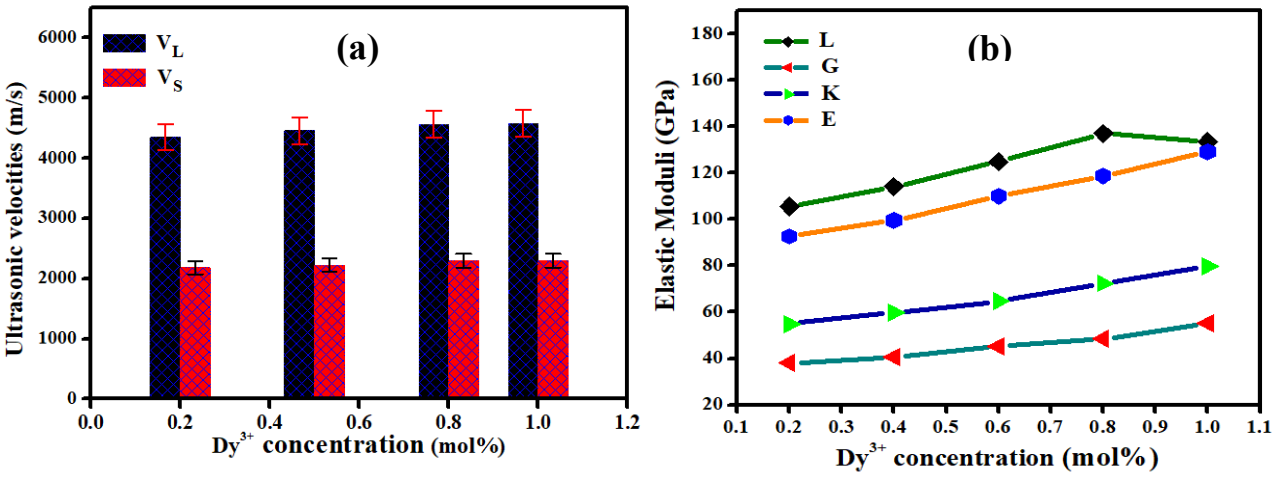

Figure 3: Variation of (a) longitudinal and shear velocity and (b) experimental elastic moduli for CSPBDy glasses.

Table 3. The ultrasonic velocities, experimental elastic moduli, Poisson's ratio (σ_{exp}), and Micro-hardness (H_{exp}) of glasses alongside reported data.

Glass samples	Velocities		Elastic moduli (GPa)				σ_{exp}	H_{exp} (GPa)	Reference
	V_L (ms^{-1})	V_S (ms^{-1})	L_{exp}	S_{exp}	K_{exp}	E_{exp}			
CSPBDy0.2	4565	2294	70.624	17.834	46.845	47.478	0.331	2.009	This study
CSPBDy0.4	4580	2300	72.578	18.303	48.174	48.738	0.331	2.039	This study
CSPBDy0.6	4640	2344	76.129	19.428	50.225	51.627	0.329	4.344	This study

SLUJST
Sule Lamido University Journal of Science & Technology Vol. 9 No. 1&2 [May, 2024], pp. 149-158
https://doi.org/10.56471/
Online ISSN: 2736-0903
Print ISSN: 2736-089X
www.slujst.edu.ng

CSPBDy0.8	4700	2359	80.540	20.290	53.487	54.036	0.332	4.517	This study
CSPBDy1.0	4328	2417	75.100	23.400	43.900	59.700	0.270	–	This study
SmZnBSLS1	5525	2985	105.885	30.906	64.677	79.978	0.294	–	Cheong et al., (2022)
TZnSm0.01	3392	1946	55.466	17.986	30.744	45.363	0.254	–	Tafida et al., (2024)

Note: SmZnBSLS: zinc-borosilicate glasses; TZnSm: zinc tellurite.

3.3.2 Theoretical Makishima-Mackenzie's and Rocherulle Model

The elastic moduli and their derivatives were computed numerically using the Makishima-Mackenzie (MM) model, and the results are presented in Table 4. It's noticeable that both the packing density and dissociation energy of the CSPBDy glasses vary with increasing Dy^{3+} concentration. The packing density values increased from 0.496 to 0.513 cm^3/mol. This observed increase in packing density is linked to the rise in density, indicating an enhancement in the compactness and rigidity of the glasses (Tafida et al., 2024). However, it's demonstrated that the inclusion of Dy^{3+} leads to an increase in the dissociation energy per unit volume (G_t) of CSPBDy glasses from 22.337 to 29.790 kJ/m^3. This physical transformation is attributed to the replacement of B2O3, which has a lower dissociation energy of 95.5 kJ/cm^3, with Dy^{3+}, which has a higher dissociation energy of 160.3 kJ/cm^3 (Adamu et al., 2022a). Furthermore, the evaluated elastic moduli are depicted in Figure 4. L_{thMM} ranges from 105.590 to 133.494 GPa, S_{thMM} from 37.991 to 55.184 GPa, K_{thMM} from 54.935 to 79.974 GPa, and E_{thMM} from 92.622 to 129.004 GPa. Similarly, Poisson's ratio values increased from 0.220 to 0.232, and the micro-hardness, H_{thMM}, from 7.092 to 9.860 GPa (Table 4). The trends of all the computed parameters are in good agreement with the experimental results.

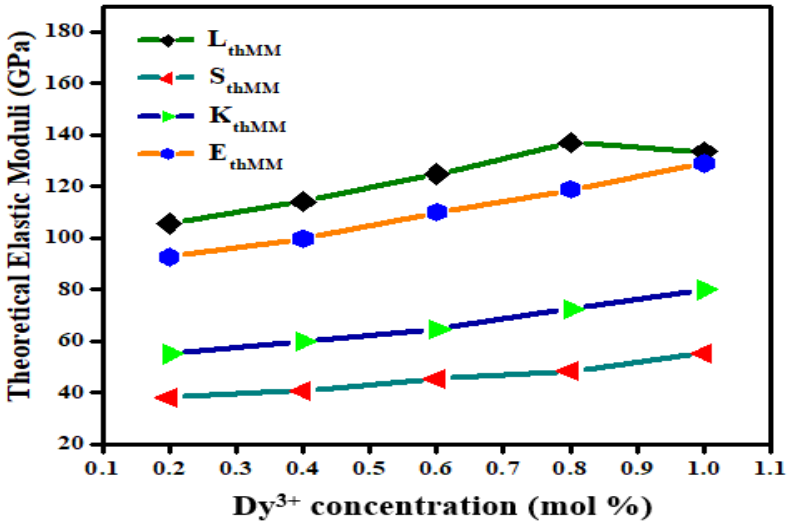

Fig. 4: M-M model based Elastic Moduli for CSPBDy glasses.

Table 4: The packing density, disassociation energy, theoretical elastic moduli Poisson's ratio and Micro-hardness of CSPBDy glasses based on MM model.

Glass samples	V_t (cm^3mol^{-1})	G_t (KJ/m^3)	Elastic moduli (GPa)				σ_{thMM}	H_{thMM} (GPa)
			L_{thMM}	S_{thMM}	K_{thMM}	E_{thMM}		
CSPBDy0.2	0.496	22.337	105.590	37.991	54.935	92.622	0.220	7.092
CSPBDy0.4	0.503	23.665	114.107	40.684	59.875	99.513	0.224	7.486
CSPBDy0.6	0.506	26.001	124.858	45.220	64.580	109.988	0.226	8.260
CSPBDy0.8	0.510	27.850	136.949	48.395	72.438	118.741	0.228	8.776

Sule Lamido University Journal of Science & Technology Vol. 9 No. 1&2 [May, 2024], pp. 149-158
https://doi.org/10.56471/
Online ISSN: 2736-0903
Print ISSN: 2736-089X
www.slujst.edu.ng

CSPBDy1.0	0.518	29.790	133.494	55.184	79.934	129.004	0.232	9.860

Furthermore, the theoretical values of packing density, elastic moduli, Poisson ratio and micro-hardness computed via Rocherulle model are tabulated in Table 5. From Table 5, it can be observed that the packing density increases from 0.509 to 0.528 cm^3/mol when Dy^{3+} ion roused from 0.2 to 1 mol%. The increase in the packing density might be due to the decrease in the interatomic spaces resulting from the formation of more bridging oxygens (BOs) with the formation of more BO_4 structural units in the glass network (Adamu et al.,2022a; Cheong et al., 2022). Besides, similar trend as demonstrated in Makishima-Mackenzie's (MM) model for disassociation energy, elastic moduli, alongside other related entities observed in this model.

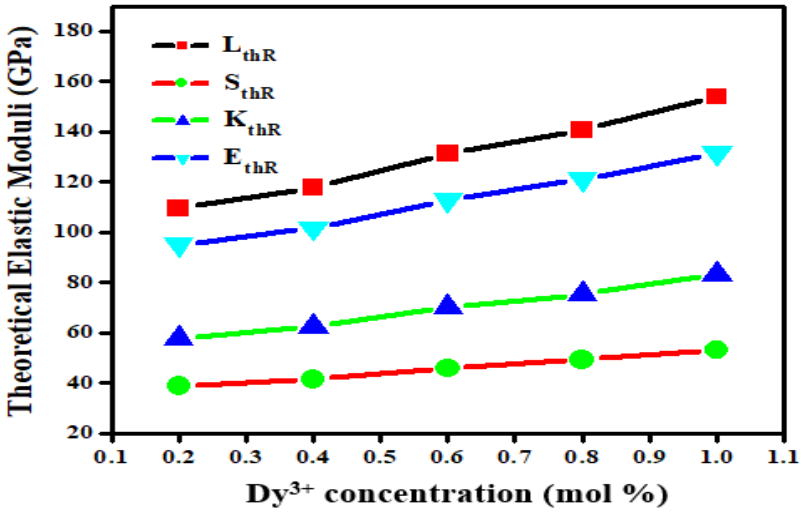

Figure 5: Rocherulle Model Based Elastic Moduli for CSPBDy glasses.

Table 5: The packing density, theoretical elastic moduli, Poisson's ratio and Micro-hardness of CSPBDy **glasses** based on Rocherulle Model

Glass samples	C_t (cm^3mol^{-1})	Elastic moduli (GPa)				σ_{thR}	H_{thR} (GPa)
		L_{thR}	S_{thR}	K_{thR}	E_{thR}		
CSPBDy0.2	0.509	109.542	38.759	57.876	95.058	0.227	7.054
CSPBDy0.4	0.514	117.672	41.373	62.522	101.689	0.230	7.447
CSPBDy0.6	0.519	131.219	45.880	70.061	112.853	0.232	8.197
CSPBDy0.8	0.520	140.837	49.150	75.320	121.091	0.233	8.749
CSPBDy1.0	0.528	153.951	53.189	83.050	131.495	0.237	9.326

3.3.3 Correlation of some selected experimental and theoretical mechanical parameters

The correlation between experimental and theoretical values of Young's modulus, Poisson's ratio, and Micro-hardness for CSPBDy glasses was investigated. To validate the findings, plots of experimental and theoretical Young's modulus (Figure 6a), Poisson's ratio (Figure 6b), and micro-hardness (Figure 6c) as functions of Dy3+ content are presented. It is evident that data evaluated using the Rocherulle model exhibit higher values than those from the Makishima-Mackenzie model. Despite this, the values from the Makishima-Mackenzie model are closer to the experimental data than those from the Rocherulle model. However, theoretical values are notably closer to

Sule Lamido University Journal of Science & Technology Vol. 9 No. 1&2 [May, 2024], pp. 149-158
https://doi.org/10.56471/
Online ISSN: 2736-0903
Print ISSN: 2736-089X
www.slujst.edu.ng

each other than to the experimental values. This consistency in theoretical values may be attributed to the beneficial effects of packing density and dissociation energies compared to ultrasonic velocities (Rocherulle et al., 1989; Tafida et al., 2024). Therefore, these findings suggest that the Makishima-Mackenzie model is more suitable for estimating the aforementioned quantities of CSPBDy glasses.

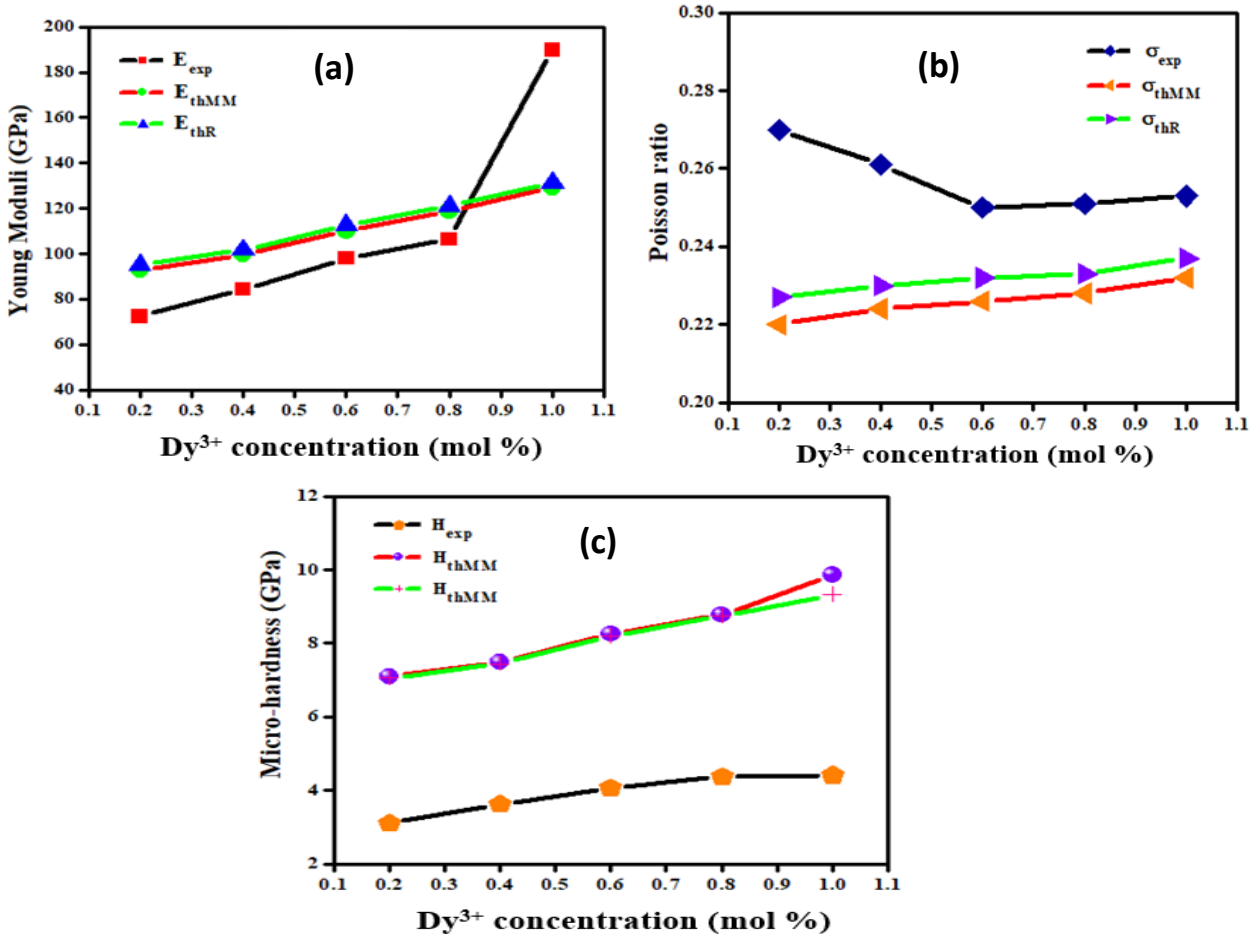

Figure 6: Comparison between experimental and theoretical values of (a) Young's modulus (b) Poisson's ratio and (c) Micro-hardness against Dy^{3+} contents (mol%)

4. Conclusion

In conclusion, a novel series of CSPBDy glasses has been successfully synthesized and characterized. Our results reveal an increase in glass density and a decrease in molar volume with higher Dy_2O_3 content. This observation indicates that Dy^{3+} acts as a network modifier, altering the glass structure by reducing non-bridging oxygen (NBOs) and enhancing the compactness of the glass network. Both ultrasonic velocities and elastic moduli exhibit this trend. Moreover, theoretical data from both the MM and Rocherulle models are consistent with experimental findings. Furthermore, a thorough comparison between experimental and theoretical data reveals that the elastic moduli data derived from the Makishima-Mackenzie model align more closely with experimental results compared to those from the Rocherulle model.

References

Online ISSN: 2736-0903
Print ISSN: 2736-089X
www.slujst.edu.ng

Abdullahi, I., Hashim, S., Ghoshal, S. K., & Ahmad, A. U. (2020). Structures and Spectroscopic Characteristics of Barium-sulfur-telluro-borate Glasses: Role of Sm^{3+} and Dy^{3+} Co-activation. *Materials Chemistry and Physics*, *247*, 122862.

Adamu, S. B., Halimah, M. K., Chan, K. T., Muhammad, F. D., Nazrin, S. N., Scavino, E., Kamaruddin, S. A., Az'lina, A. H., Ghani, N. A. M. M., Az'lina, A. H., & Ghani, N. A. M. M. (2022a). Structural, Prediction and Simulation of Elastic Properties for Tellurite Based Glass Systems doped with nano and micro Eu_2O_3 particles via Artificial Neural Network Model. *Journal of Materials Research and Technology*, 17, 586–600. https://doi.org/10.1016/j.jmrt.2022.01.035

Adamu, S. B., Halimah, M. K., Chan, K. T., Muhammad, F. D., Nazrin, S. N., & Tafida, R. A. (2022b). Eu^{3+} ions doped Zinc Borotellurite Glass System for White Light Laser Application: Structural, Physical, Optical Properties, and Judd-Ofelt theory. *Journal of Luminescence*, 250, 119099.

Alqarni, A. S., Hussin, R., Alamri, S. N., & Ghoshal, S. K., (2020). Spectral features of Ho^{3+}-doped boro-Phosphate Glass-Ceramics: Role of Ag Nanoparticles Sensitization. *Journal of Luminescence*, *223*, 117218.

Alharshan, G. A., Eke, C., Ibraheem, A. A., Alrowaili, Z. A., Sriwunkum, C., & Al-Buriahi, M. S. (2022). Hardness, Elastic Properties, and Radiation Shielding Performance of the CdO-P_2O_5-NiO Glass System. *Journal of Electronic Materials*, *51*(10), 5808-5817.

Bengisu, M., (2016). Borate Glasses for Scientific and Industrial Applications: A Review. *Journal of Materials Science*, 51(5). 2199-2242.

Bulus, I., Dalhatu, S. A., Hussin, R., Wan Shamsuri, W. N., & Yamusa, Y. A., (2017). The Role of Dysprosium Ions on the Physical and Optical Properties of Lithium-borosulfophosphate glasses. *International Journal of Modern Physics B*, *31*(13). 1750101.

Cheong, Wei Mun, Zaid, M. H. M., Matori, K. A., Fen, Yap Wing, Tee, Tan Sin, Loh, Zhi Wei, & Schmid, Siegbert. (2022). Structural, Elastic and Mechanical Analysis of Samarium Doped Zinc-Borosilicate Glass. Optik, 267, 169658.

Danmallam, I. M., & Bulus, I. (2020). Correlation of Optical and Mechanical Properties of Silver Nanoparticles Sensitized Europium Doped Phosphate Glasses. *Science Proceedings Series*, 2(2), 147–55.

Danmallam, I. M., Ghoshal, S. K., Ariffin, R., Bulus, I., & Yamusa, Y. A. (2021). Correlation of Mechanical Properties and Crystal Field Parameters of Europium-Doped Magnesium–Zinc–Sulfophosphate Glasses. *Indian Journal of Physics*, 95(11), 2453–61.

Halimah, M. K., Ami Hazlin, M. N., & Muhammad, F. D. (2018). Experimental and Theoretical Approach on the Optical Properties of Zinc Borotellurite Glass Doped with Dysprosium Oxide. *Spectrochimica Acta - Part A: Molecular and Biomolecular Spectroscopy*, 195, 128–35.

Rocherulle, J., Ecolivet, C., Poulain, M., Verdier, P., & Laurent, Y., (1989). Elastic Moduli of Oxynitride Glasses: Extension of Makishima and Mackenzie's Theory. *Journal of non-crystalline solids*, *108*(2). 187-193.

Razak, N. A., Hashim, S., Mhareb, M. H. A., Alajerami, Y. S. M., Azizan, S. A., & Tamchek, N. (2016). Impact of Eu^{3+} ions on Physical and Optical Properties of Li_2O-Na_2O-B_2O_3 Glass. *Chinese Journal of Chemical Physics*, *29*(3), 395.

Karthikeyan, P., Arunkumar, S., Annapoorani, K., & Marimuthu, K. (2018). Investigations on the Spectroscopic Properties of Dy^{3+} ions Doped Zinc Calcium Tellurofluoroborate Glasses. *Spectrochimica Acta Part A: Molecular and Biomolecular Spectroscopy*, *193*, 422-431.

Tafida, R. A., Thakur, S., Onimisi, M. Y., Garba, S., Adamu, S. B., Shitu, I. G., & Lakin, I. I. (2024). Unvelling the Elastic Properties of Samarium Oxide Zinc Tellurite - Based Glasses : Judd - Ofelt Intensity Parameters Through Structural, Experimental, and Theoretical Studies. *Optical and Quantum Electronics*, 56(964), 1–32.

Yaacob, S. S., Mohd-Noor, F., Mawlud, S. Q., Aziz, S. M., Yusoff, N. M., Yusof, N. N., & Safaai, S. S., (2023). Correlation Between Structural and Mechano-Optical Response of Modified Europium in Magnesium Borotellurite Glass. *Journal of Non-Crystalline Solids*, *600*, 122010.